13

Changes of the crystalline texture and resistivity of Ti films under ion bombardment

© R.V. Selyukov,[1] I.I. Amirov,[1] M.O. Izyumov,[1] V.V. Naumov,[1] L.A. Mazaletskiy[2]

[1] Valiev Institute of Physics and Technology of RAS, Yaroslavl Branch,
150007 Yaroslavl, Russia
[2] Demidov State University,
150003 Yaroslavl, Russia
e-mail: rvselyukov@mail.ru

Received May 30, 2023
Revised July 27, 2023
Accepted July 28, 2023

Crystalline texture, microstructure and resistivity of ion irradiated 12−41 nm Ti films are investigated. Ion bombardment was carried out in Ar plasma by applying negative bias 20−30 V to the films. It is found that this treatment leads to the formation of [100] texture in films having initially mixed [100] + [001] texture. The less the film thickness and the higher the bias the less treatment time is required for the [100] texture formation. Ion irradiation of 12 and 22 nm films using bias 30 V leads to the increase of interplanar distances in surface normal direction by 3% and the decrease of film resistivity by 14−20%.

Keywords: thin films, titanium, ion bombardment, plasma, crystalline texture, resistivity, X-ray diffraction.

DOI: 10.61011/TP.2023.10.57458.139-23

Introduction

Thin textured Ti films are used as an adhesive layer when deposited on various substrates of TiN [1,2] coatings, Al [3,4] films, AlN [5–7], Pt [8,9], ferromagnetic films [10]. As a rule, a film α-Ti with a fiber texture [001] is used, the arrangement of atoms and interatomic distances in the Ti (001) planes are similar to those for the (111) Al, Pt and (001) AlN planes. In all of the above cases, the strengthening of the texture of the Ti layer leads to texture strengthening, and consequently, the operational properties of films and multilayer systems deposited on it.

The desired type and sharpness of the texture of Ti films are obtained by adjusting the parameters of deposition processes, in particular, bombardment of the growing film with Ti ions or inert gases is used [1–3,11–17]. Such bombardment occurs when a constant or radio-frequency (RF) bias is applied to the substrate, or when an ion source is used [1,3,17]. Accelerating voltages in the first case usually do not exceed hundreds of volts, in the second case the accelerating voltage is units-tens of kilovolts. At the same time, the impact of low-energy bombardment with inert gas ions carried out after deposition on the texture of Ti and other metals films has been poorly studied. Meanwhile, such a procedure carried out in argon plasma can be applied, for example, to prepare adhesive layers Ti [18], stress changes in metal films [19], their phase composition [20] and resistivity [20,21].

The aim of this work was to determine the effect of low-energy bombardment with Ar ions on the texture of Ti films with a thickness of 12−41 nm. Ion bombardment was carried out in an argon plasma of an RF inductive discharge, the accelerating voltage was changed due to the supply of RF bias of various power to the studied samples. The results of studies of the texture of Ti films processed at a bias on a substrate of 30 V were published in [22], this paper presents the results of studies of texture and resistivity for films processed at displacements of 20−30 V.

1. Experiment

Ti films with a thickness of $h = 12$, 22, 32 and 41 nm were deposited on a wafer Si(100) coated with thermal SiO_2 thickness 1 μm by magnetron sputtering. The deposition was carried out in magnetron sputterer Alcatel SCR 651 „Tetra“ setup at room temperature with floating potential on the substrate. The pressure Ar during deposition was 0.2 Pa, RF power on the target was 300 W, the distance between the target and the substrate was 100 mm.

After deposition, the films were subjected to a series of ion-plasma treatments (IPT), which were carried out in an RF inductive discharge reactor in argon plasma, described in detail in [23]. During the IPT, the Ar pressure in the reactor was 0.08 Pa, RF power supplied to the inductor was 800 W. The ion current density was 7.4 mA/cm^2. The films were subjected to a series of four IPT with a duration of 30 min each, at different values of RF bias on the substrate, which led to the appearance of a constant negative potential relative to the housing of 20, 25 and 30 V. According to [24] the following relation is valid between the average energy of argon ions E_{ion} and bias U for the conditions of ion bombardment carried out in our study: $E_{\text{ion}} = -eU$. Thus, it can be argued that the ion energies of Ar were 20−30 eV. The samples were glued with vacuum grease to an aluminum substrate holder, which was located with

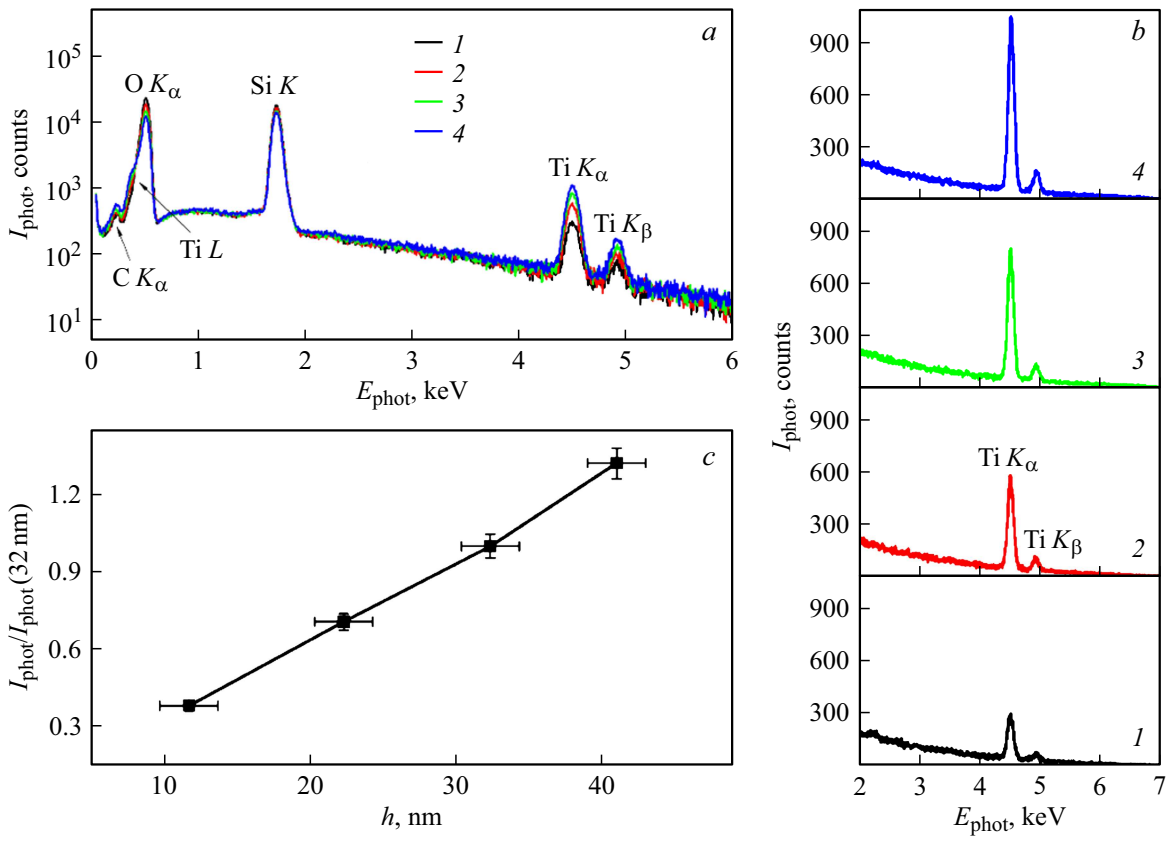

Figure 1. *a* — energy-dispersive spectra of samples with as-deposited films Ti: *1* — spectrum for the as-deposited film thickness 12 nm, *2* — 22, *3* — 32, *4* — 41 nm; *b* — peak Ti K_α at $E_{phot} \sim 4.51$ keV on spectra for as-deposited films Ti; *c* — dependence of peak intensity Ti K_α I_{phot} on thickness of the as-deposited film Ti, normalized by the peak intensity Ti K_α of the film Ti thickness 32 nm I_{phot} (32 nm) and used as a calibration curve to determine the thickness of the treated films Ti.

a 0.1mm gap above the water-cooled electrode. Helium gas was supplied to the gap at pressure 10^3 Pa, due to the thermal conductivity of which the substrate holder with the sample is cooled, so during the IPT their temperature did not exceed 40°C.

Diffractograms were taken using a DRON-3M diffractometer in the Bragg–Brentano geometry using copper anode tube, Cu K_β line was eliminated by a pyrographite crystal monochromator, Cu $K_{\alpha 2}$ line was eliminated using the modified Rachinger method [25]. The resistivity ρ was measured using a four-probe method using a DC source P321 and a voltmeter B7-21 at current values 0.2–2 mA, while the voltage on the samples was 7–10 mV. It was found that ρ of the original films, as well as those subjected to IPT, did not change in the intervals between IPT, which were up to several days. Thus, the effect on ρ of the oxidation of Ti films as a result of their exposure to air can be neglected. The chemical composition of the films was studied using energy dispersive X-ray spectroscopy (EDX) and Auger electron spectroscopy (AES). The AES spectra of the thin near-surface region of the film were taken at the PHI-660 installation at an electron probe energy of 10 keV in residual vacuum $5.3 \cdot 10^{-6}$ Pa.

The thickness of the films before and after the IPT was measured using EDX spectra according to the method proposed in [26]. EDX spectra of the as-deposited films with $h = 12–41$ nm, as well as a calibration sample — 32 nm thick Ti film, deposited under the same conditions as the studied films were recorded using INCAx-act detector (Oxford Instruments) of Supra-40 SEM (Carl Zeiss) at an accelerating voltage of 7 kV. The variation of the electron beam current values in each series of measurements with a calibration sample did not exceed 1%. The size of the scan area was the same in all measurements. The energy dispersion spectra for the as-deposited samples are shown in Fig. 1, *a, b*. The intensities of the K_α-line Ti (~ 4.51 keV), $I_{phot}(h)$ and I_{phot} (32 nm) were measured for the as-deposited samples with h thick Ti films and the calibration sample, respectively, while the background was not subtracted from the spectra. The thicknesses of the as-deposited films were measured using SEM images of the cleavage of the corresponding samples. Next, the calibration curve — dependence of $I_{phot}(h)/I_{phot}$ (32 nm) on h was constructed, which was approximated by a piecewise linear function (Fig. 1, *c*). The EDX spectra of the studied (with film of unknown thickness x, [nm]) and calibration samples were recorded under the same condi-

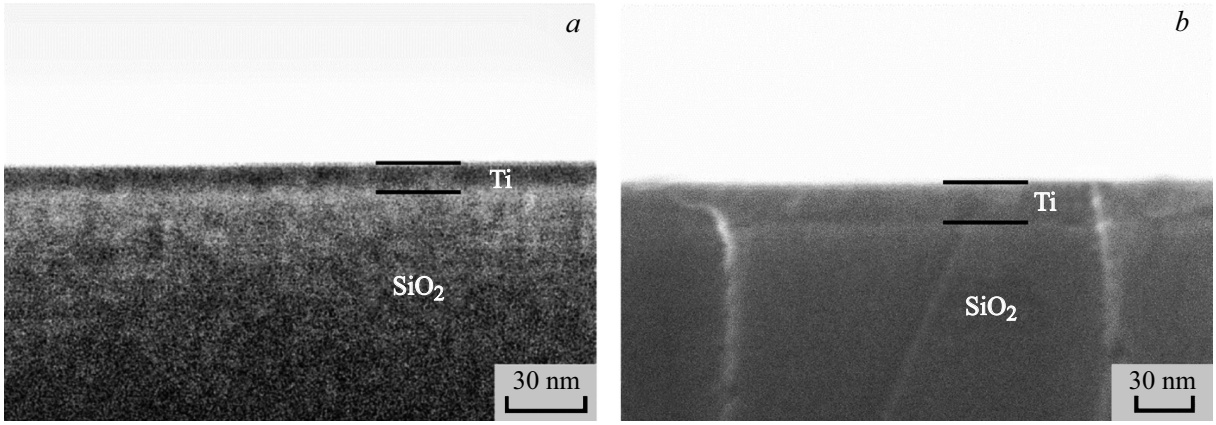

Figure 2. SEM images of cleavage of the as-deposited samples with Ti films 12 (*a*) and 22 nm (*b*).

tions as for the as-deposited samples. The film thickness was determined using a calibration curve in magnitude $I_{\text{phot}}(x\,\text{nm})/I_{\text{phot}}(32\,\text{nm})$. SEM images of cleavage for the as-deposited samples with films with a thickness of 12 and 22 nm are shown in Fig. 2. It can be seen that in both cases the films are dense, with a roughness negligible in comparison with the thickness of the film.

The morphology of the surface of the films was studied using the Supra-40 SEM, the images were obtained in the secondary electron mode at the angle of incidence of the electron beam on the surface of the film equal to 70°.

2. Results and discussion

2.1. EDX and AES studies

7 kV accelerating voltage was used for EDX spectra recording, such a value was chosen to register Ti *K*-lines located on the spectrum in the region 4.5−5 keV. Ti *L*-lines located on 400−460 eV, overlap with O K_α-line, therefore cannot be used for analysis. A weak $K_{\alpha 1}$ line *C* at 277 eV, and also intense lines Si, O, Ti are presented on EDX spectra of all samples. There are no lines Ar ($K_{\alpha 1}$ at 2958 eV, $K_{\alpha 2}$ at 2956 eV, doublet $K_{\beta 1,3}$ at 3191 eV). The source of the Si and O lines is SiO_2 of the substrate. The observation of intense peaks of the substrate material indicates that when recording the spectrum, the excitation depth exceeded the thickness of the film; thus, the recording conditions of the spectra allow measuring *h*.

The thicknesses of Ti films were measured before and after each series of IPT using EDX spectra. It was found that a near-surface layer with a thickness of 4−5 nm was removed in the first batch, as a result of a series of four 30 V IPT, a series of 25 V IPT resulted in thinning of the Ti film by 1−2 nm, there was no Ti thinning after a series of 20 V IPT.

The spectra of AES films with an initial thickness of 12 and 22 nm were recorded before and after the series of 30 V IPT. The chemical composition of the near-surface region of Ti films with a thickness of 1−2 nm was analyzed. It was found that C and O are present on the surface before and after the IPT, in addition to Ti. Si signal appears after IPT. The composition of the near-surface areas of films of different thicknesses is approximately the same before IPT: the proportion of Ti is equal to 16−18 at.%, C — 35−39 at.%, O — 45−47 at.%. The composition for different films is also the same after IPT, but the O fraction becomes smaller, and C fraction becomes larger. Ti-fraction is 12−13 at.%, C fraction is 50 at.%, O fraction is 28−29 at.%, Si fraction is 9 at.%. The Si signal appears only after the IPT, which can be explained by the formation of pores in the film as a result of ion sputtering. The presence of O is associated with the presence of Ti oxide on the surface and decreases as a result of IPT, which can be explained by the removal of the oxide film during sputtering.

2.2. XRD studies

Fig. 3 shows the diffractograms of Ti films with $h = 12$ and 22 nm, initial and subjected IPT in different modes. Only the peak of Si 200 substrate at $2\theta \sim 33°$, and also the maxima at $2\theta \sim 35$ and 38°, related to Ti are present in diffractograms in $2\theta = 20-68°$ angle range. The peak at $2\theta \sim 35°$ is the maximum 100 of phase α-Ti with a hexagonal densely packed lattice. The peak at $2\theta \sim 38°$ can be both a maximum 002 of α-Ti and a maximum 110 of the high-temperature phase β-Ti having a volume-centered cubic lattice. Data on the presence of the β-phase in Ti thin films deposited by magnetron sputtering at a temperature below the phase transition point are available in the literature [28]. A maximum 200 of phases β-Ti should be recorded if the film contains β-Ti grains with planes (110) parallel to the surface, then when the sample is tilted by an angle $\psi \sim 45°$ and the detector position $2\theta \sim 55.5°$. However, on diffractograms and pole figures taken in the vicinity of the angles $\psi = 45°$ and $2\theta = 55.5°$, this peak is absent. At the same time, for $\psi \sim 61°$ and $2\theta \sim 40°$, a peak of 101 corresponding to grains of α-Ti with planes parallel to the substrate (001) is recorded. Consequently, the presence of

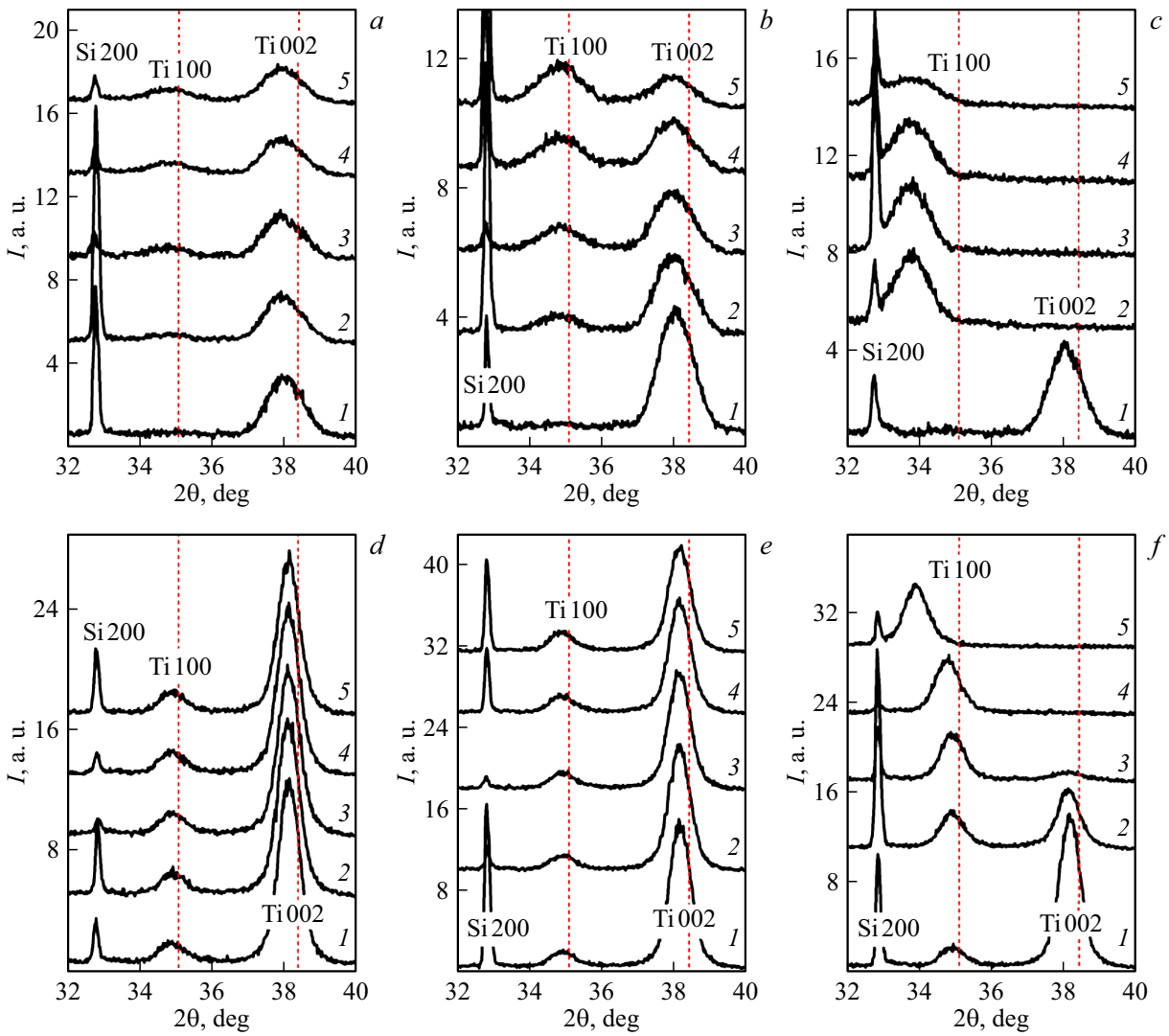

Figure 3. Diffractograms of Ti films of initial thickness 12 (*a–c*) and 22 nm (*d–f*) before and after IPT with an bias on the substrate 20 (*a, d*), 25 (*b, e*) and 30 V (*c, f*). *1* — the as-deposited film, *2* — after the first IPT, *3* — after the second IPT, *4* — after the third IPT, *5* — after the fourth IPT. The duration of each IPT is — 30 min. The substrate peak is Si 200 at $2\theta \sim 33°$, peak Ti 100 at $2\theta \sim 34–35°$, peak Ti 002 at $\sim 38°$. Vertical lines indicate the positions of peaks 100 and 002 for the bulk α-Ti [27].

β-Ti in the films is not confirmed, and the peak at $2\theta \sim 38°$ is the diffraction maximum of 002 phase α-Ti.

Thus, only α-phase Ti with mixed texture is present in all as-deposited films [100] + [001]. Fig. 3 shows that 30 V IPT lead to significant texture changes: the 002 peak disappears, while the maximum of 100 increases. 100 peak is at $2\theta \sim 34°$ in 12 nm film subjected to 30 V IPT, and also in 22 nm film subjected to a series of four 30 V IPT. No data on Ti phases with such diffraction maximum were found in the literature. Also, this peak cannot be attributed to the phases of any Ti compounds, since it is absent on the diffractograms of 22–41 films nm after the first IPT, while, according to the AES, the content of impurities in the near-surface region of the films does not depend on their initial thickness. The interplanar distance measured in the normal direction to the substrate is d_{100} in 12 nm film after the first 30 V IPT is greater than that in the original film by 3%. This result is similar to those presented in [29,30], where it was found that the interplanar distance increased by 6.7% in Nb film with a decrease of grain size from 10 to 5 nm reached. This result was explained by the stresses acting in the film in [29]. The sizes of coherently diffracting domains (CDD) were estimated in this paper using the Scherrer formula for peaks Ti 002 and 100 without taking into account the hardware function and microdeformations, the results for 30 V IPT are presented in Fig. 4. It was found that the CDD of the as-deposited samples of Ti 002 and Ti 100 peaks increased by about 50% with an increase of film thickness from 12 to 41 nm. The size of CDD also decreases during IPT. The interplanar distances d_{100} and d_{001} in the direction normal to the surface were measured from the positions of the diffraction peaks (Fig. 5). These values

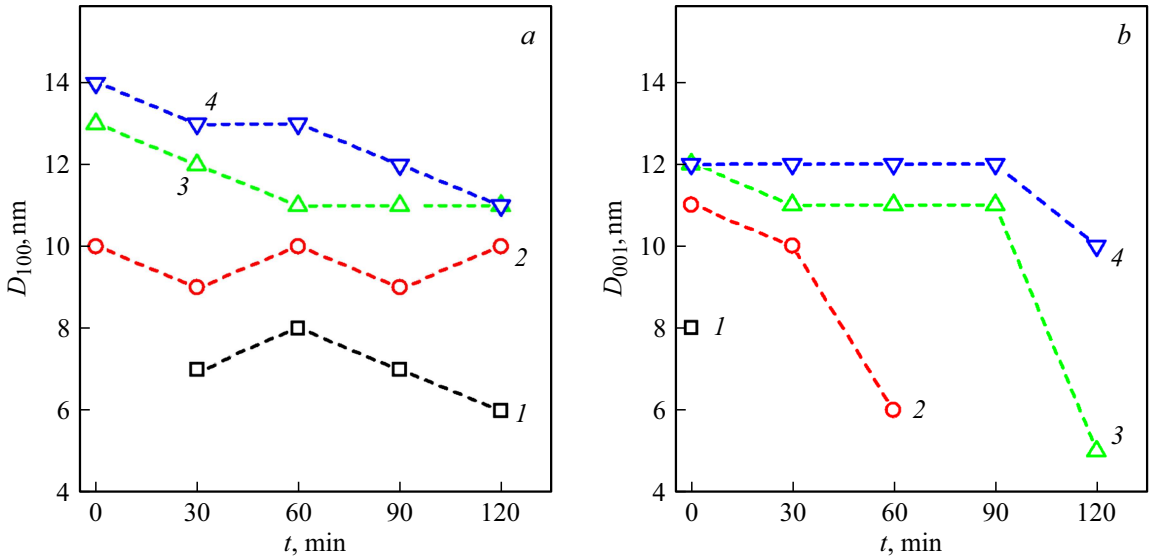

Figure 4. The dependence of the size of the CDD on the time of the IPT in the mode 30 V. The value D_{100} (a) is calculated using the profile Ti 100, the value D_{001} (b) is calculated using the profile Ti 002. *1* — film of initial thickness 12 nm, *2* — 22, *3* — 32, *4* — 41 nm.

are $d^0_{100} = 2.56$ Å and $d^0_{001} = 4.68$ Åfor bulk Ti [5,7,14,15]. The values of d_{100} and d_{001} obtained in this work for the as-deposited and processed films exceed the values for the bulk material, which indicates compressive stress in the film plane. d_{100} and d_{001} increase with a decrease of the thickness of the as-deposited film, which indicates an increase of compressive stress and is consistent with the results of [29,30]. d_{100} and d_{001} increase as a result of the IPT in 20 and 25 V modes for films with a thickness of 12 nm, they slightly change in 22–41 nm thick films , d_{100} and d_{001} increase of films 12 and 22 nm as a result of IPT in 30 V mode. The stresses in the films, estimated using the formula $\sigma = E/2\mu(d_{001}-d^0_{001})/d^0_{001}$ [31], where E — Young's modulus, μ — Poisson's ratio, give values for the original films from ~ 1.0 GPa for the film 41 nm to ~ 1.7 GPa for film 12 nm. The stress calculation using the formula $\sigma = E/2\mu(d_{100}-d^0_{100})/d^0_{100}$ gives an abnormally large stress value of ~ 6 GPa in 12 and 22 nm films subjected to a series of IPT in the 30 V mode. Thus, it can be argued that the maximum at $2\theta \sim 34°$ is the peak of 100 α-Ti. This change in the interplanar distance cannot be explained by the implantation of argon into the film, since Ar was not found in the films as a result of EDX and AES measurements, in addition, $2\theta \sim 34°$ peak does not appear on the diffractograms of 32 and 41 nm films. The intensity of the Ti 100 peak increases with an increase of the total IPT time as a result of the IPT 20 V only for 12 nm film, the diffractogram of 22 nm film does not change. The result of the IPT series 25 V is similar to the result of 20 V IPT, however, Ti 100 peak intensity relative to the peak intensity Ti 002 increases faster with an increase of the total IPT time in 12 nm film.

Thus, the ion bombardment of the Ti film leads to changes in the crystal texture. As a quantitative characteristic of the texture, it is convenient to use the relative integral intensity of $I_{100}/(I_{100}+I_{002})$ peak [11,15]. Fig. 6, a–c shows the dependencies of the parameter $I_{100}/(I_{100}+I_{002})$ on the time of the IPT t for different modes. It can be seen that grains with planes (001) oriented parallel to the substrate dominate in 12 nm thick as-deposited film, the proportion of [100] oriented grains increases with an increase of the thickness of the as-deposited film. It is known that grains with planes (001) oriented parallel to the substrate have a minimum surface energy [32–34], the elastic strain energy [11,32,34] is minimal in grains with planes (100) parallel to the substrate. Thus, an increase of the proportion of [100] oriented grains with an increase of the film thickness is probably attributable to an increase of stresses (Fig. 5) and the elastic strain energy caused by them. It was found that [001] oriented grains disappear and a texture is formed [100] in the 30 V mode, after the first IPT in the 12 nm film. The same effect in 22 nm film is achieved as a result of three consecutive IPT, the texture [100] becomes dominant after four IPT in 32, nm film. At the same time, the series of IPT with a total duration of 120 min slightly increases the parameter $I_{100}/(I_{100}+I_{002})$ in 41 nm film. 20 and 25 V IPT slightly change the proportion of [100] oriented grains in22–41 nm films, but this proportion increases in 12 nm film, and this increase is the greater the greater is the bias on the substrate.

The increase of the proportion of [100] oriented grains as a result of IPT cannot be explained only by the preferential sputtering of [001] oriented grains. In this case, the intensity of the peak 002 as a result of the IPT would decrease, which does not correspond to the results obtained. This can be confirmed by analyzing the change in the absolute values of the integral intensity of peaks on diffractograms. Fig. 6, d shows a change of I_{100} depending on the thickness

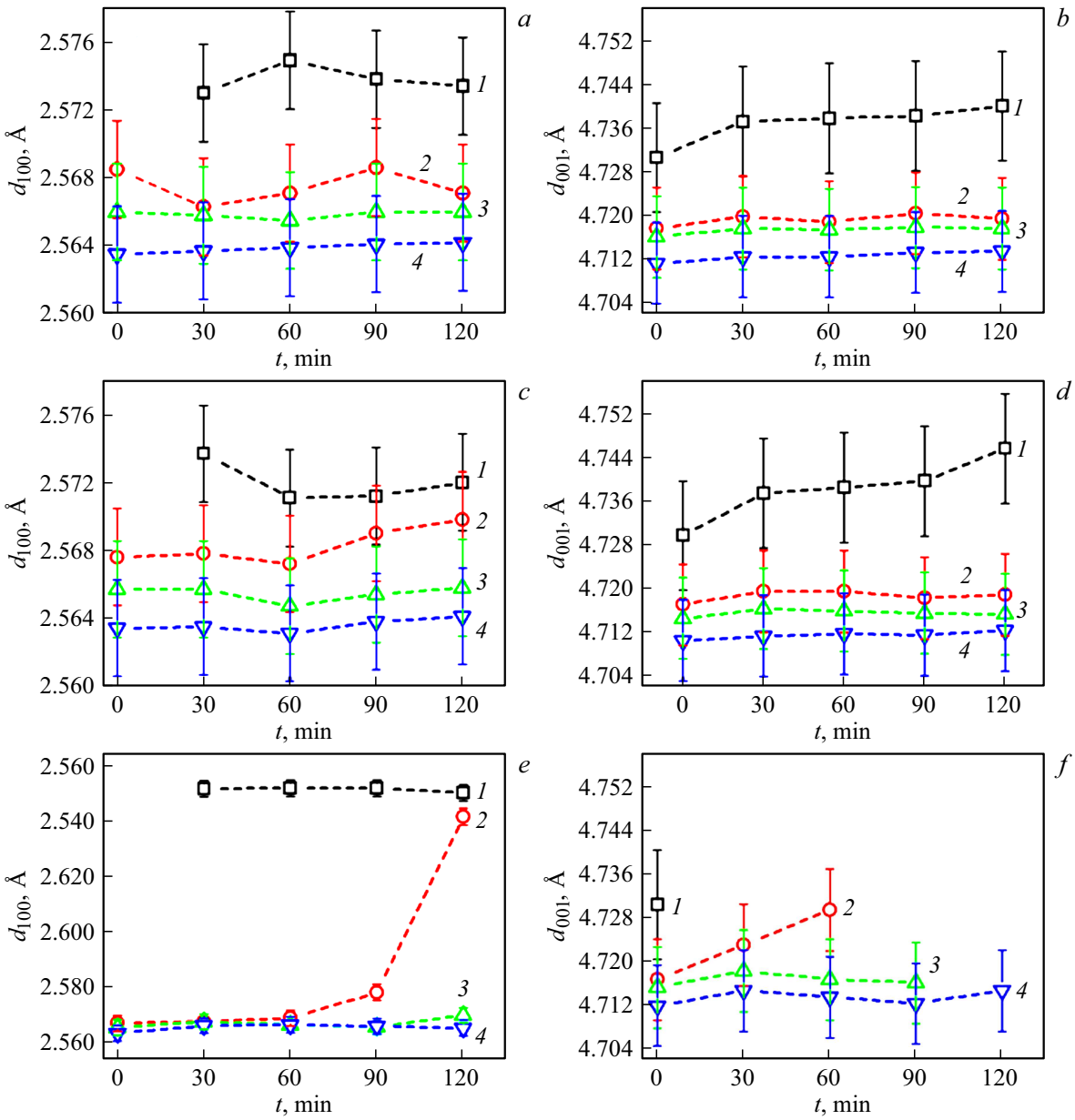

Figure 5. Dependence of interplanar distances d_{100} (*a, c, e*) and d_{001} (*b, d, f*) in the direction normals to the substrate from the IPT time for modes 20 (*a, b*), 25 (*c, d*), 30 V (*e, f*). *1* — film of initial thickness 12 nm, *2* — 22, *3* — 32, *4* — 41 nm.

of the original film for the series of 30 V IPT. The integral intensity of 100 I_{100} peak at first sharply increases in this series in 12 nm films, and then the intensity weakens, which is explained by a decrease of the thickness of the film as a result of sputtering. I_{100} increases throughout the series in 22 nm film. Since all films are thinned during the IPT process, the increase of I_{100} in 12 and 22 nm films can only be explained by the transformation of [001] oriented grains into [100] oriented ones. The rate of increase of the number of [100] oriented grains in 22 nm film as a result of such transformation exceeds the rate of decrease of their number as a result of thinning. I_{100} attenuation occurs in 32 and 41 nm films, which is explained by thinning of the films.

The film thinning does not exceed 1–2 nm in series of 20 and 25 V IPT, while I_{100} in 32 and 41 nm films does not change in the series of IPT, I_{100} increases by 5–6 times in 12 nm films, I_{100} does not change in 22 nm film in 20 V mode and it increases by 1.5 times in 25 V mode. As in the case of 30 V IPT, in this case, the growth of I_{100} is explained by the restructuring of the grains, leading to an increase of the proportion of [100] oriented grains.

It was mentioned above that the texture of [100] in α-Ti films is attributable to stress. The following qualitative explanation for the reorientation of grains as a result of IPT can be proposed based on this fact. Earlier, [19,35] showed that IPT leads to an increase of compressive stress in Cr films, which was explained by the diffusion of atoms from

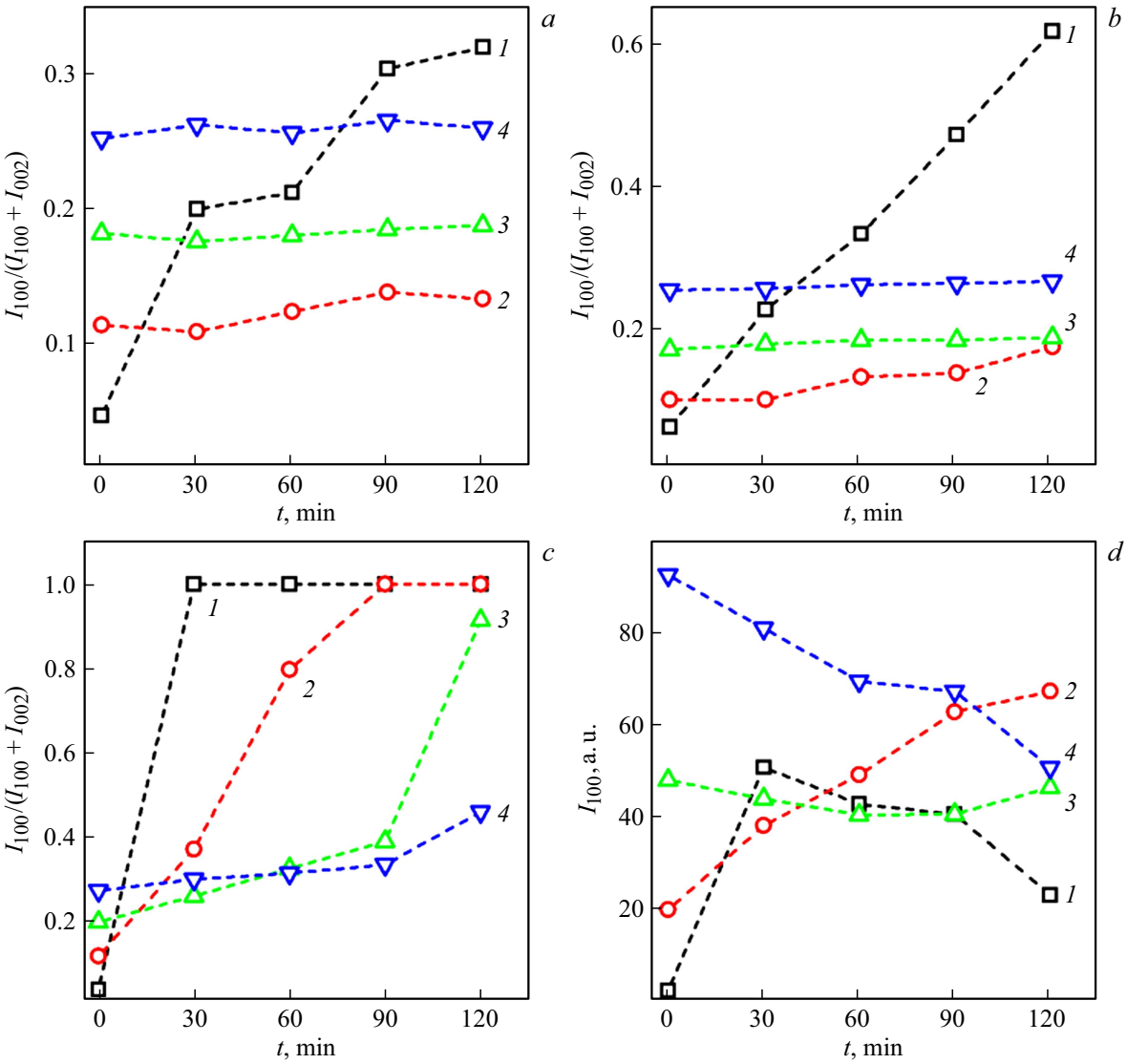

Figure 6. The dependence of the relative intensity of peak Ti 100 $I_{100}/(I_{100}+I_{002})$ on the total IPT time t in 20 (*a*), 25 (*b*), 30 V mode (*c*). Ti 100 I_{100} peak intensity depending on IPT time in 30 mode,V (*d*). *1* — Ti film with an initial thickness of 12 nm, *2* — 22, *3* — 32, *4* — 41 nm.

the surface into the grain boundaries within the framework of the model of compressive stress generation proposed in [36]. Ion-induced compressive stress in this system can be the driving force that changes the texture of Ti film. An increase of d_{100} and d_{001}, and consequently, increase of stress in the film plane, with an increase of the IPT time indicates an increase of compressive stress in the film plane. Fig. 5 shows that 20–30 V IPT leads to an increase of d_{001} in 12 nm films, IPT 30 V increase the stresses in 22 nm film, the same stresses change weakly in 32 and 41 nm films. This result generally correlates with the increase of the fraction of [100]-oriented grains. The formation of a (100) texture in Ti films was observed in [11,12] as a result of ion bombardment, carried out, however, during deposition; this result was also explained by strong compressive stress in [11].

It should be noted that a similar effect was observed in [32] when the addition of deuterium to the atmosphere during Ti deposition led to the formation of [100] texture, but no increase of stress was observed. The formation of the [100] texture was explained in [32] by a decrease of the mobility of adatoms on the (100) and (001) planes due to deuterium adsorption, which made the growth of [100] oriented grains preferable due to the lower packing density of atoms in the (100) planes. In our case, the analysis of the chemical composition of the near-surface areas of the film indicates the removal of oxygen as a result of ion bombardment, as well as the absence of argon after it, therefore, the effect of adsorption of impurities on the restructuring of grains is not confirmed.

The increase of the rate of texture change with an increase of bias on the substrate, as well as with a decrease of the

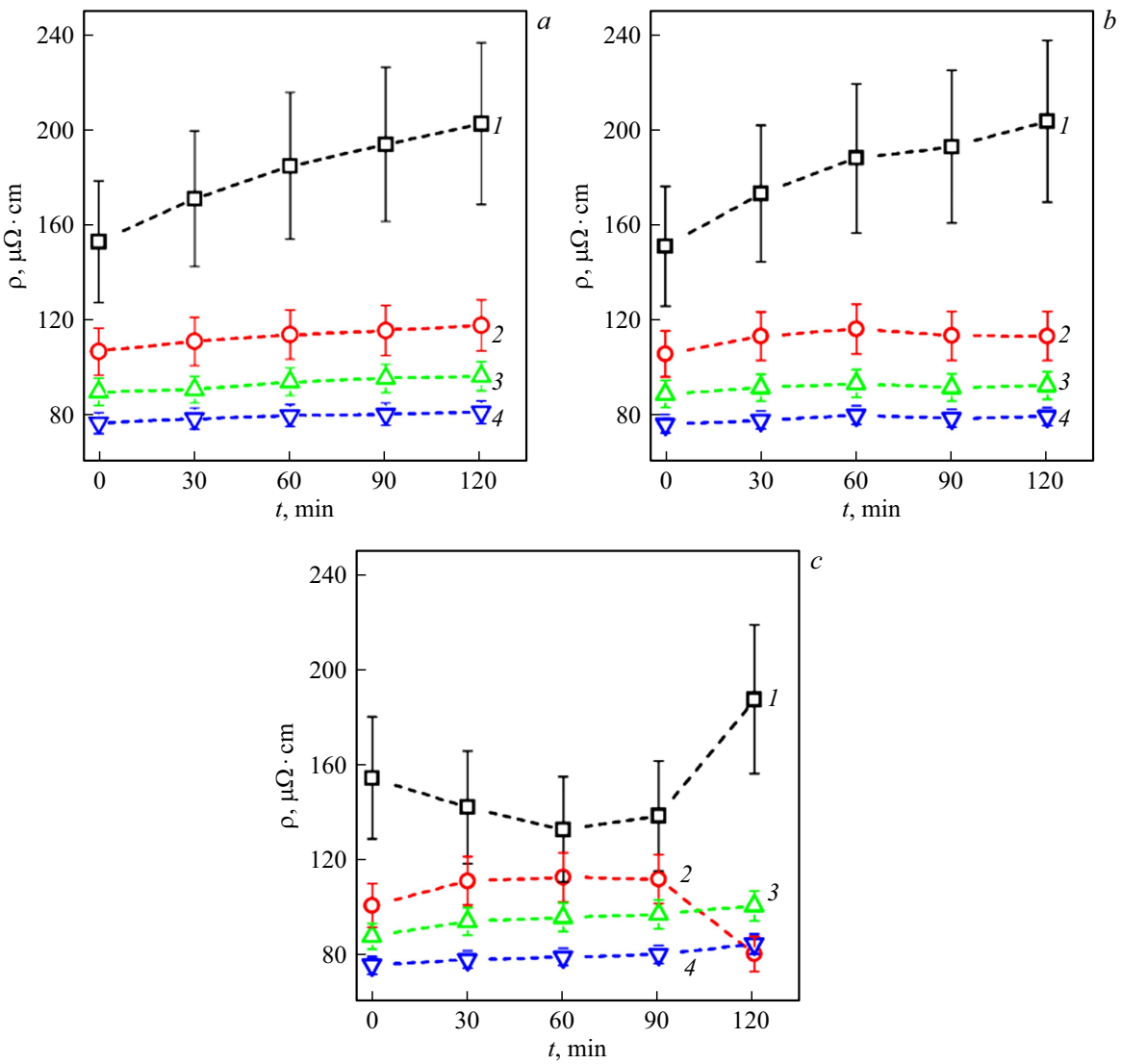

Figure 7. Dependence of ρ Ti films on the IPT time in 20 (*a*), 25 (*b*), 30 V modes (*c*). *1* — film of initial thickness 12 nm, *2* — 22, *3* — 32, *4* — 41 nm.

thickness of the film, can be qualitatively explained within the framework of the theory proposed in [36], according to which, mobile adatoms on the surface diffuse into the grain boundaries during the deposition of the film which results in the generation of compressive stress. Ion bombardment of the surface of the Ti film leads to the sputtering of atoms from the near-surface layers, while some of the atoms do not leave the surface. As a result, the concentration of adatoms on the surface increases. An increase of the average energy of Ar ions contributes to an increase of the mobility of adatoms, which, in turn, increases their diffusion length in the case of surface and grain-boundary diffusion. For the same value of the diffusion length of adatoms, the restructuring of a thinner film occurs faster. The migration of adatoms to grain boundaries will accelerate with an increase of the total area of these boundaries. Figure 4 shows that the CDD size decreases with a decrease of the thickness of the as-deposited film. Smaller CDD sizes in the case of the thinner film mean the larger total area of grain boundaries, which in turn means the increase of the atomic flux density during grain boundary diffusion.

Thus, a significant (by 3%) increase of the interplanar distance d_{100} in 12 and 22 nm films after the series of 30 V IPT can be explained by the cumulative effect of a decrease of the size of the CDD (Fig. 4) as a result of IPT [29,30] and an increase of compressive stress.

2.3. Measurement of the resistivity of Ti films

Figure 7 shows the dependence of ρ Ti films on the total IPT time t. It can be seen that the smaller the film thickness is the greater is the increase of ρ in 20 and 25 V modes. There is no noticeable thinning of the film in these modes, the size of the CDD also does not change, so the increase of ρ can be explained by the introduction of radiation defects into the near-surface layer. ρ varies

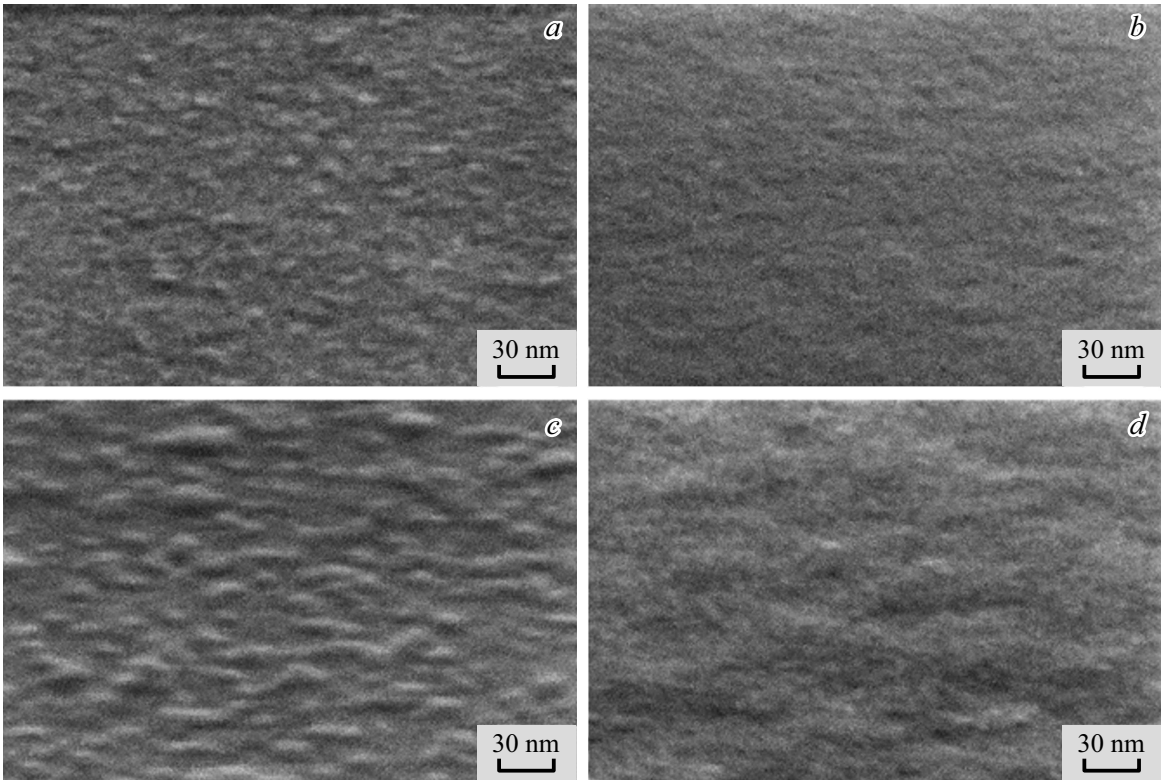

Figure 8. SEM images of 12 (a, b) and 22 nm Ti films (c, d), the as-deposited films (a, c) and films subjected to a series of 30 V IPT (b, d).

slightly in 30 V mode in 32 and 41 nm films, while there are the decreasing areas on the dependence of ρ on t in 12 and 22 nm films that coincide in time of the IPT with the shift of the position of Ti 100 peak to the position $2\theta \sim 34^\circ$. The value of ρ itself significantly exceeds that for bulk material, increasing with the decrease of the film thickness, which is typical for thin films and is attributable to the scattering of charge carriers at grain boundaries and on the surface. ρ exceeds the resistivity of the bulk Ti by 1.8 times in 41 nm as-deposited film and by 3.6 times in 12 nm as-deposited film. The decrease of ρ in 12 nm film after the first two 30 V IPT is 14%, a further increase of ρ is associated with its thinning during sputtering. The reduction of ρ in 22 nm film as a result of the fourth IPT in 30 V series is 28%; thus, ρ in this film is 20% less than ρ in the same film before the treatments. The reduction of ρ by 14 and 20% in 12 and 22 nm films are reproduced in repeated experiments with Ti films deposited and treated under similar conditions.

It is known that monocrystalline Ti is characterized by anisotropy ρ, which, however, does not exceed 7% [37]. Thus, the observed decrease of ρ can not be explained only by a change of texture. The removal of the oxide film as a result of IPT also cannot explain the reduction of ρ, since such a reduction, firstly, does not occur as a result of IPT for other film thicknesses, and secondly, the removal of oxide occurs during each IPT, and reduction of ρ is observed only after certain IPT. As a result of 30 V IPT, both the CDD (Fig. 4) and the film thickness decrease, which gives contributions to an increase of ρ at corresponding sites depending on duration of IPT.

Figure 8 shows the SEM images for the film with an initial thickness of 12 and 22 nm before and after the series of 30 V IPT. It can be seen that the roughness of 12 nm film decreases as a result of IPT, and the lateral dimensions of the objects that make up the surface also decrease. In the case of 22 nm film, the lateral dimensions of the objects that make up the surface increase, and the roughness does not change noticeably. The result obtained for 22 nm film is consistent with the results obtained for Pt film subjected to IPT in modes similar to those used in this study [38]. A reduction of the roughness of the film as a result of IPT may be responsible for a decrease of ρ, however, it seems that the change in surface morphology during IPT is monotonous, while ρ decreases within a relatively short period of IPT duration. Since the decrease of ρ in case of 12 and 22 nm films coincides in time with a strong shift of the peak position 100, which also occurs abruptly, it can be assumed that it is attributable to a change of the electronic structure of the material due to changes of interatomic distances. The decrease observed in [39] and measured along the direction [001] ρ for a Gd crystal also having a hexagonal densely packed lattice was explained by a change of the parameters of the crystal

lattice. A decrease of ρ of Gd samples subjected to pressure of several GPa was also observed in [40]. The above stress values for films treated in the 30 V, 12 and 22 nm mode are consistent with the value of the pressure used in [40].

Conclusion

It is shown that the proportion of [100]-oriented grains increases as a result of ion-plasma treatment of 12−41 nm Ti films with a complex texture consisting of [100]- and [001]-oriented grains, when the bias 20−30 V is applied to the samples. This effect is more pronounced the smaller the film thickness and the greater the bias on the substrate. The observed restructuring of the texture is explained by the occurrence of compressive stress in the film during ion-plasma treatment. The interplanar distance in the normal direction to the substrate increases by 3% as a result of treatment of 12 and 22 nm films by 30 V. The resistivity of these films is by 14−20% less than before treatment.

Funding

The investigation was supported by Program № FFNN-2022-0017 of the Ministry of Science and Higher Education of Russia for Valiev Institute of Physics and Technology of RAS. SEM, EDX and AES studies were performed using the equipment of the Facilities Sharing Centre „Diagnostics of Micro- and Nanostructures“ with the financial support of the Ministry of Education and Science of the Russian Federation.

Conflict of interest

The authors declare that they have no conflict of interest.

References

[1] J.-H. Huang, Ch.-H. Ma, H. Chen. Surf. Coat. Technol., **200**, 5937 (2006). DOI: 10.1016/j.surfcoat.2005.09.005
[2] W. Zhang, L. Yi, J. Tu, P. Chang, D. Mao, J. Wu. J. Electron. Mater., **34**, 1307 (2005). DOI: 10.1007/s11664-005-0254-7
[3] D.M. Li, F. Pan, J.B. Niu, M. Liu. J. Electron. Mater., **34**, 1053 (2005). DOI: 10.1007/s11664-005-0095-4
[4] S. Okasha, Y. Sekine, S. Sasaki, Y. Harada. Thin Solid Films, **732**, 138784 (2021). DOI: 10.1016/j.tsf.2021.138784
[5] J. Xiong, H.-Sh. Gu, K. Hu, M.-Z. Hu. Int. J. Miner. Metall. Mater., **17**, 98 (2010). DOI: 10.1007/s12613-010-0117-y
[6] A.T. Tran, O. Wunnicke, G. Pandraud, M.D. Nguyen, H. Schellevis, P.M. Sarro. Sens. Act. A Phys., **202**, 118 (2013). DOI: 10.1016/j.sna.2013.01.047
[7] M.A. Signore, A. Taurinoa, M. Catalano, M. Kim, Z. Che, F. Quaranta, P. Siciliano. Mater. Des., **119**, 151 (2017). DOI: 10.1016/j.matdes.2017.01.035
[8] R. Toyama, S. Kawachi, J. Yamaura, Y. Murakami, H. Hosono, Y. Majima. Jpn. J. Appl. Phys., **59**, 075504 (2020). DOI: 10.35848/1347-4065/ab9627
[9] K.A. Vorotilov, O.M. Zhigalina, V.A. Vasil'ev, A.S. Sigov. Phys. Solid State, **51** (7), 1337 (2009). DOI: 10.1134/S106378340907004X
[10] A.K. Sahoo, J.A. Chelvane, J. Mohanty. J. Mater. Sci.: Mater. Electron., **32**, 7567 (2021). DOI: 10.1007/s10854-021-05471-y
[11] D.L. Ma, Y.T. Li, Q.Y. Deng, B. Huang, Y.X. Leng, N. Huang. Int. J. Mod. Phys. B, **33**, 1940017 (2019). DOI: 10.1142/S0217979219400174
[12] M.J. Jung, K.H. Nam, L.R. Shaginyan, J.G. Han. Thin Solid Films, **435**, 145 (2003). DOI: 10.1016/S0040-6090(03)00344-4
[13] W. Zhang, L. Yi, K.T. Yue, M. P. Chang, J. Wu. J. Mater. Sci: Mater. Electron., **17**, 931 (2006). DOI: 10.1007/s10854-006-0046-8
[14] Y.-L. Liu, F. Liu, Q. Wu, A.-Y. Chen, X. Li, D. Pan. Trans. Nonferrous Met. Soc. China, **24**, 2870 (2014). DOI: 10.1016/S1003-6326(14)63420-8
[15] B.G. Priyadarshini, Sh. Aich, M. Chakraborty. Bull. Mater. Sci., **37**, 1691 (2014). DOI: 10.1007/s12034-014-0722-x
[16] B. Wu, Y. Yu, J. Wu, I. Shchelkanov, D.N. Ruzic, N. Huang, Y.X. Leng. Vacuum, **150**, 144 (2018). DOI: 10.1016/j.vacuum.2018.01.039
[17] Y. He, J. Zhang, W. Yao, D. Li, X. Teng. Appl. Surf. Sci., **255**, 4484 (2009). DOI: 10.1016/j.apsusc.2008.11.053
[18] K. Kamoshida, Y. Ito. J. Vac. Sci. Technol. B, **15**, 961 (1997). DOI: 10.1116/1.589515
[19] A.S. Babushkin, I.V. Uvarov, I.I. Amirov. Tech. Phys., **63** (12), 1800 (2018). DOI: 10.1134/S1063784218120228
[20] R.V. Selyukov, I.I. Amirov, V.V. Naumov. Russ. Microelectron., **51** (6), 488 (2022). DOI: 10.1134/S1063739722700081
[21] I.I. Amirov, R.V. Selyukov, V.V. Naumov, E.S. Gorlachev. Russ. Microelectron., **50** (1), 1 (2021). DOI: 10.1134/S1063739721010030
[22] R.V. Selyukov, M.O. Izyumov, V.V. Naumov, L.A. Mazaletskiy. Tech. Phys. Lett., **48** (15), 25 (2021). DOI: 10.21883/TPL.2022.15.53816.18890
[23] I.I. Amirov, M.O. Izyumov, V.V. Naumov. J. Surf. Investig., **10** (4), 855 (2016). DOI: 10.1134/S1027451016040236
[24] I.I. Amirov, M.O. Izyumov, V.V. Naumov, E.S. Gorlachev. J. Phys. D: Appl. Phys., **54**, 065204 (2021). DOI: 10.1088/1361-6463/abc3ed
[25] R. Delhez, E.J. Mittemeijer. J. Appl. Cryst., **8**, 609 (1975). DOI: 10.1107/S0021889875011466
[26] W.E. Sweeney Jr., R.E. Seebold, L.S. Birks. J. Appl. Phys., **31**, 1061 (1960). DOI: 10.1063/1.1735746
[27] R.R. Pawar, V.T. Deshpande. Acta Cryst., **A24**, 316 (1968). DOI: 10.1107/S0567739468000525
[28] J. Kong, H. Shen, B. Chen, Z. Li, W. Shi, W. Yao, Zh. Qi. Thin Solid Films, **207**, 51 (1992). DOI: 10.1016/0040-6090(92)90100-P
[29] R. Banerjee, E.A. Sperling, G.B. Thompson, H.L. Fraser, S. Bose, P. Ayyub. Appl. Phys. Lett., **82**, 4250 (2003). DOI: 10.1063/1.1582361
[30] D. Hazra, S. Datta, M. Mondal, J. Ghatak, P.V. Satyam, A.K. Gupta. J. Appl. Phys., **103**, 103535 (2008). DOI: 10.1063/1.2924332
[31] E.G. Fu, Y.Q. Wang, M. Nastasi. J. Phys. D, **45**, 495303 (2012). DOI: 10.1088/0022-3727/45/49/495303
[32] R. Checchetto. Thin Solid Films, **302**, 77 (1997). DOI: 10.1016/S0040-6090(96)09552-1
[33] J. Chakraborty, K. Kumar, R. Ranjan, S.G. Chowdhury, S.R. Singh. Solid State Phenom., **160**, 109 (2010). DOI: 10.4028/www.scientific.net/SSP.160.109

[34] F.J. Jing, T.L. Yin, K. Yukimura, H. Sun, Y.X. Leng, N. Huang. Vacuum, **86**, 2114 (2012). DOI: 10.1016/j.vacuum.2012.06.003
[35] A. Babushkin, R. Selyukov, I. Amirov. Proc. SPIE, **11022**, 1102223 (2019). DOI: 10.1117/12.2521617
[36] E. Chason, J.W. Shin, S.J. Hearne, L.B. Freund. J. Appl. Phys., **111**, 083520 (2012). DOI: 10.1063/1.4704683
[37] M.E. Day, M. Delfino, J.A. Fair, W. Tsai. Thin Solid Films, **254**, 285 (1995). DOI: 10.1016/0040-6090(94)06259-N
[38] R.V. Selyukov, M.O. Izyumov, V.V. Naumov. J. Surf. Investig., **14** (4), 777 (2020). DOI: 10.1134/S1027451020040321
[39] F.C. Zumsteg, F.J. Cadieu, S. Marcelja, R.D. Parks. Phys. Rev. Lett., **25**, 1204 (1970). DOI: 10.1103/PhysRevLett.25.1204
[40] R.A. Stager, H.G. Drickamer. Phys. Rev., **133**, A830 (1964). DOI: 10.1103/PhysRev.133.A830

Translated by Ego Translating